Modelling and Simulation of the Power Take-Off System for a Hinge-Barge Wave-Energy Converter

G. Nolan[1] *, M. Ó Catháin[1], J. Murtagh[2] and J.V. Ringwood[1]

[1]Dept. of Electronic Engineering
National University of Ireland, Maynooth
Co. Kildare, Ireland

[2]Machine & System Designers
Maynooth Road, Celbridge
Co. Kildare, Ireland

* corresponding author
Email: gary.nolan@eeng.may.ie

Abstract

The McCabe Wave Pump (MWP) has possibilities for the conversion of wave energy into electrical energy and the production of potable water. However, in order to optimise the dynamics and operation of this device in the face of a wide variety of sea conditions, a number of important control issues must be addressed. The first step, which is addressed in this paper, is the production of a dynamical model of the MWP, which can provide a basis for both control design and simulation. Since the power take-off (PTO) system provides the main damping in the system, the paper places particular emphasis on the PTO model and how it couples to the main rig dynamics. The control problem formulation is also briefly addressed.

1 Introduction

The McCabe Wave Pump is classified as a hinged-barge wave energy converter (WEC), and is designed for wave regimes typically occurring 1-2 km offshore. A considerable number of studies, both theoretical [1, 2, 3] and experimental (scale [4] and prototype [5] models) and have been conducted on the McCabe Wave Pump system. The work documented herein builds on this previous body of work by developing a mathematical model for the full hydraulic power take-off device [10], and considers its effect on the behaviour of the overall system model previously developed by Kraemer [1].

The development of an accurate mathematical model is required in order to understand the dynamics of the system and can also feed back into the structural design of the MWP. The model is also vital in providing a basis for model-based computer control design, which will be used to continuously adjust a variety of actuators in order to optimise the process behaviour. A prototype MWP is currently deployed off the South West coast of Ireland for sea trials and an important next step is the incorporation of feedback control technology in the device.

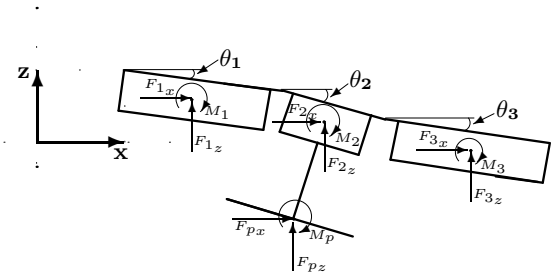

Figure 1: Schematic of the 2D MWP System Model

The paper is organised as follows: Section 2 outlines the overall MWP dynamics and highlights the effect of the PTO system. The PTO model is developed in Section 3, with the specific coupling mechanism between MWP and PTO models documented in Section 4. Finally, the control problem is formulated in Section 5 and conclusions drawn in Section 6.

2 Wave-Barge Interaction

The model used to describe the motions of the MWP system is that developed by Kraemer [1, 2] at Johns Hopkins University. Previously, McCormick [3] modelled a two-barge system using an energy based method, considering heave and pitch degrees of freedom, and assuming small pitching angles of the barges. Kraemer uses an alternative forced-based method to formulate the non-linear equations of motion of a hinged-barge system with an arbitrary number of barges and inertial plates, considering surge as well as heave and pitch motions, and without assuming small pitch angles. A brief summary of Kraemer's model is given here, together with discussion of features relevant to its use in control design.

2.1 Governing Equations

In modelling the MWP, Kraemer [1] considers planar motions in 5 degrees of freedom, namely heave and surge of the bow of the first barge, and three pitch angles (see Figure 1). All forces and moments acting on an individual barge are expressed via translational (two) and rotational (one) equations of motion. The 9 equations of motion in 9 unknowns, for the system of 3 barges acting independently of each other, are reduced to a set of 5 equations in 5 unknowns by considering kinematic constraints at the linkages between barges and by eliminating internal forces (note that the moments due to the PTO are treated as external to the hinge-barge system). This equation set may be expressed in matrix form as:

$$I\ddot{q} = F \tag{1}$$

where $q = [x, z, \theta_1, \theta_2, \theta_3]^T$ is the displacement vector, with the state variables x, z, θ_1, θ_2 & θ_3 as indicated in Figure 1. $I \in \Re^{5\times5}$ is the inertial matrix. Its diagonal elements correspond to surge, heave and pitch of the system, while its off-diagonal elements are due to inertial coupling between surge-pitch, heave-pitch and pitch-pitch modes. The added-mass elements are included in the inertial matrix.

$F = [F_1, F_2, F_3, F_4, F_5]^T$ is the force vector, where
$F_1 = f_1(F_{i_x}, F_{p_x}), i = 1, 2, 3$
$F_2 = f_2(F_{i_z}, F_{p_z}), i = 1, 2, 3$
$F_3 = f_3(M_1, F_{i_x}, F_{i_z}, F_{p_x}, F_{p_z}, sin\theta_1, cos\theta_1),$
$\quad i = 1, 2, 3$
$F_4 = f_4(M_2, M_p, F_{i_x}, F_{i_z}, F_{p_x}, F_{p_z}, sin\theta_2, cos\theta_2),$
$\quad i = 2, 3$
$F_5 = f_5(M_3, F_{3_x}, F_{3_z}, F_{p_x}, F_{p_z}, sin\theta_3, cos\theta_3)$
with
$F_{i_x} = F_{i_{scatt_x}} + F_{i_{rad_x}} + F_{i_{stat_x}}$
$F_{i_z} = F_{i_{scatt_z}} + F_{i_{rad_z}} + F_{i_{stat_z}} + F_{i_{grav}}$
$M_i = M_{i_{scatt}} + M_{i_{rad}} + M_{i_{stat}} + M_{i_{grav}} + M_{i_{PTO}}$
$F_{p_x} = F_{p_{scatt_x}} + F_{p_{rad_x}}$
$F_{p_z} = F_{p_{scatt_z}} + F_{p_{rad_z}} + F_{p_{grav}} + F_{p_{visc}}$
$M_p = M_{p_{scatt}} + M_{p_{rad}} + M_{p_{visc}}$

with i indicating barge number, F and M indicating force and moment respectively, and subscripts indicating the following:

scatt:	Scattering Force/Moment
rad:	Radiation Force/Moment
stat:	Hydrostatic Force/Moment
grav:	Gravitational Force

Of particular interest here is the term $M_{i_{PTO}}$. This represents the moment on each barge due to the PTO. Kraemer assumes that this moment may be modelled as a linear rotational damper, i.e.

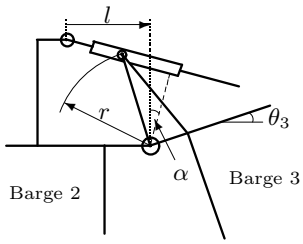

Figure 2: Schematic of the hinge assembly

$$M_{i_{PTO}} = c(\dot{\theta}_i - \dot{\theta_{i+1}}) \tag{2}$$

where c is the rotational damping coefficient.
In the work presented in this paper, the translational force on reciprocating pumps due to this moment is treated as the input to a bond graph model of the PTO system.

Murtagh [10] gives the relation between the moment and the translational force as:

$$F_{i_{PTO}} = \frac{M_{i_{PTO}}}{r\cos(\theta_{i+1} + \alpha)} \tag{3}$$

where $\alpha = \tan^{-1}\left(\frac{r(1-cos\theta_i)}{l-rsin\theta_i}\right)$ and l and r are displacements associated with the hinge assembly as indicated in Figure 2. Note that Figure 2 illustrates the representative case of the linkage between barges 2 and 3, with barge 2 having zero pitch angle.

2.2 Assumptions

Linear wave theory (see, for example [7]) is assumed in Kraemer's treatment of the hydrodynamic forces on the hinge-barge system, allowing the forces to be decomposed into incident, scattering and radiation forces. Incident waves are assumed to be sinusoidal.

Regular seas have been assumed, i.e. monochromatic waves. When structural dynamics of a WEC are linear, it is possible to account for irregular waves by using the principle of superposition to add the effects of each frequency in the incident wave. However, for the case of the MWP system, this will not be possible as the equations of motion indicate non-linear structural dynamics. It may be necessary to develop a time-domain model of the hydrodynamic forces, of the type developed by Jefferys [8] or Yu and Falnes [9].

Kraemer [1] assumes that the PTO may be adequately modelled as a linear rotational damper, with inertia being negligible in comparison. The damping force coefficient is not fixed, but vary de-

pending on values of parameter in the PTO model. This is further addressed in Section 4.

2.3 Features of the equations of motion

The scattering force is considered as the forcing input to the system. Here, we have used Kraemer's [1] definition of scattering force, i.e. that force resulting from the addition of forces due to the incident wave and scattering velocity potentials, ϕ_0 and ϕ_7 respectively. Since ϕ_7 represents the incident incident wave scattered (diffracted and reflected) by the stationary body, the scattering force is independent of the body displacements, and may be considered as the forcing input to the system.

The outputs of the wave/barge subsystem are the motion state variables q, $\dot{q}$, $\ddot{q}$. These are used as inputs to the PTO system (Section 4) and the control system (Section 5).

Overall, it is clear to see that significant nonlinearity is present in the system via the trigonometric relationships discussed in Section 2.1 as well as the nonlinearities introduced by valve characteristics and the dependence on the PTO damping value on variables within the PTO subsystem.

3 Modelling the PTO System

This section details the mathematical model of the PTO system explaining the approach taken, the completed model, any assumptions made and concludes with some simulation results and considerations for possible model usage.

3.1 The PTO System

The full PTO system [6, 10] can be broken down into a number of subsystems as indicated in Figure 3. The overall input to the PTO system is the mechanical moment provided by the barge motion. The overall objective for the PTO model is therefore to provide an accurate representation of the elements in figure 3, driven by the overall system inputs and control signals. The entire PTO system, prior to the Pelton wheel has been modelled using a bond graph approach. The physical gap between the control valve and the buckets of the Pelton wheel allow it to be separated from the remainder of the PTO subsystem, for modelling purposes. However, it is still necessary to include the Pelton wheel equations in the full system model as one of the control objectives is to maximise the power delivered to the electrical generator via the Pelton wheel.

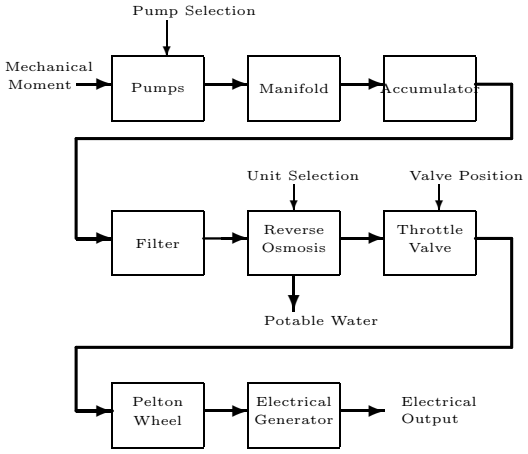

Figure 3: Block Diagram of the Power Take-Off System

3.2 The Bond Graph Model

Bond graphs [11, 12], introduced by Paynter in 1959, are based on the concept of power flow modelling and can be described as a graphical tool for capturing the common energy structures of systems [11]. The motivation behind choosing bond graphs to model the PTO system is:

- The systematic approach to creating the bond graph,
- They are visually easy to understand and to compare with other energy domains (e.g. electrical analogies),
- Ease of connection between energy domains, and
- Systematic derivation of system equations.

Figure 4 illustrates the bond graph representing the PTO system. It also contains a schematic of a simple pump, in which R_{cv} indicates the check valves that allow pumping in both directions and a rectified flow output. The sections of the bond graph labelled the fore and aft barge pumps can be thought of as one of these simple pumps. Bonds $1, 2, 3$ and $13, 14, 15$ represent the suction pipes of the fore barge pump with the effort source inputs at bond 1 and 13 representing atmospheric and depth pressure forcing water into the pipe. The '0' between bonds $3, 4, 6$ and $12, 15, 16$ represent the flow junction and single pressure point of the top and bottom chambers, respectively, of the fore barge pump. The effort source at bond 9 is the driving force ($F_{i_{PTO}}$) on the pumps from the hinge-barge supplied by the equations of motion discussed in

Section 2. It is the transformers (labelled TF) which convert this force into its corresponding hydraulic pressure and flow. This design is then repeated for the aft barge pump. Graphically, it may seem that the bond graph only contains two pumps. However, by varying parameter values, the full five pumps on board the current MWP prototype are modelled. In fact, the MWP has three pumps on the fore barge side and two pumps on the aft barge side all of which have the capability to be switched in and out. The 'switching' is achieved by changing the piston surface area in the pumps so as to represent one, two or three pumps. It is not possible to combine all five pumps together as the fore and aft barge pumps are subject to driving forces of different magnitude and phase.

The modulating resistance values of the check valves (R_{cv}) have a dual function. Firstly, the resistance value represents the check valve being open or closed and secondly, when the check valve is open, the resistance value represents any losses (pipe losses and bend losses) that need to be modelled.

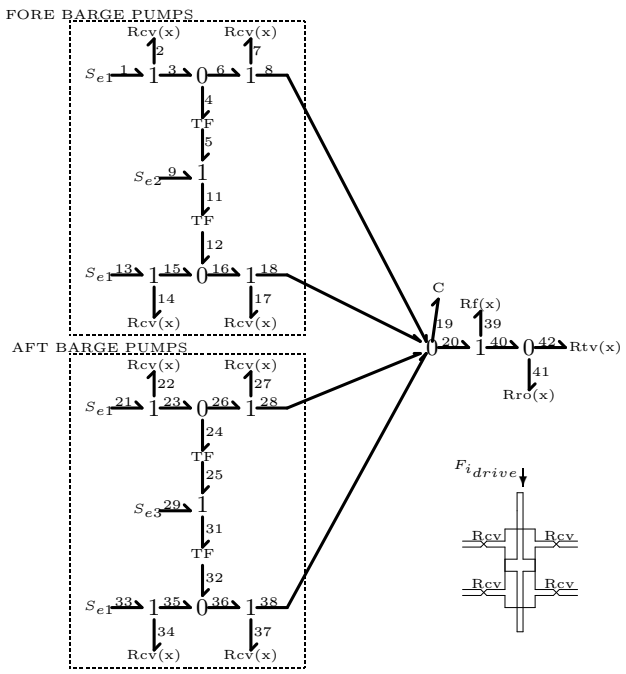

Figure 4: Bond Graph of the Power Take-Off System

The accumulator is modelled as a capacitive element (at bond 19). Capacitive elements are used to model devices that store and give up energy without loss. The constitutive relation between effort and displacement for a gas bladder type accumulator is given [13] as:

$$\triangle p = (p_0\gamma/v_0)\triangle v \tag{4}$$

giving the capacitance value, C_{acc}, as:

$$C_{acc} = (v_0/p_0\gamma) \tag{5}$$

The throttle valve and the RO system membrane are included in the bond graph as modulated resistances R_{tv} and R_{ro} respectively. The throttle valve resistance is calculated using a number of equations, with the most crucial being Darcy's equation for head loss [15].

$$H_L = \frac{KV^2}{2g} \tag{6}$$

For the throttle valve, it is the resistance coefficient (K) that changes (usually nonlinearly) with valve position. This is the primary control input which is used to maintain the operating pressure for maximum potable water output. Darcy's equation is also used to calculate the resistance value representing the filter (R_f). The resistance value of the RO membrane is calculated by manipulating the water transport equation for the rate of water through a semi-permeable membrane, given [14] as,

$$Q_w = (\triangle P - \triangle P_{osm})K_w S/d_m \tag{7}$$

with,

$$R_{ro} = \triangle P/Q_w \tag{8}$$

Again, through parameter variation, the switching in and out of multiple banks of RO membranes is modelled. Finally, the Pelton wheel (not included in the bond graph) equations, completes the full model of the PTO system, described by:

$$V_j = \sqrt{2(p_1/\rho)} \tag{9}$$

and,

$$P_h = (1/2)\rho V_j Q_{tv} \tag{10}$$

3.3 Assumptions

This PTO system model makes a number of assumptions, with the first being that there is insignificant inertance effects experienced by the fluids in the pipes. These effects are only noticed in pipes of small internal diameter or of relatively long length, of which the PTO system has none. Secondly, it has been assumed that when a pump is switched out by opening its bypass valve that negligible amounts of back pressure are felt by the barge. If, during validation, this is found not to be the case, parameters will be changed to include this effect. It is also assumed that any fouling or concentration polarization effects can be neglected as the RO system will be regularly cleaned by reverse flushing.

3.4 Formulation of PTO Equation Set

Formulation of the system equations from bond graphs gives a state space description with the state variables provided by the storage elements, in this case the accumulator. The formulation involves assigning causality to the bond graph, writing down the constitutive relations of the storage and resistive elements and then writing out and reducing the junction equations. This should yield the system equations in terms of the systems states and parameters. However, in this case there is an algebraic loop in the bond graph, with no intermediate states, from the input at bond 9 out to bond 18 and back around via bond 8 and likewise a loop in the Aft barge pumps section of the bond graph. This means that the junction equations cannot be reduced and need to be written as a set of linear equations and solved by some formal method. In this case Gaussian elimination was used and, due to the large number of junction equations, was carried out by Mathematica. Mathematica also allowed some sorting and simplification of the state equation. The bond graph approach also allows derivation of expressions for output variables that may not be state variables. This allows expressions for the pressure in the piston chambers, pressure at the accumulator, and output flows through the throttle valve and RO system, to be derived.

3.5 Simulation Results

Figures 5 and 6 illustrate sample results from a simulation of the PTO model described in the previous section. In both cases the force inputs (which in the full system model will be supplied by the MWP equations of motion) are sinusoidal. These force inputs (S_{e2} and S_{e3} on the bond graph) are of different magnitude and phase representing the different forces experienced by the pumps of the fore and aft barge.

Figure 5 contains the throttle valve and potable water outputs and also illustrates the extra smoothing effect that could be achieved by resizing the accumulator. In the simulation, accumulator two would represent an accumulator with a greater capacitance value.

Figure 6 contains a plot of the pressure in the manifold and also illustrates the effect of varying the throttle valve position. Varying the valve from position one through to position three represents reducing the valve opening and this can be seen to have the result of increasing the pressure in the manifold.

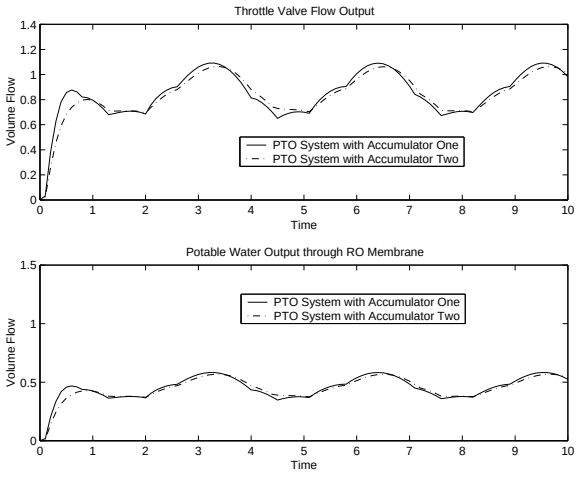

Figure 5: PTO System Flow Outputs

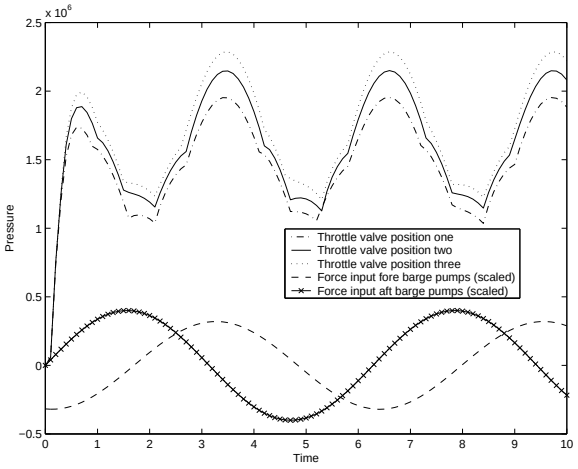

Figure 6: Manifold Pressure

3.6 PTO Model Usage

Once validated with data from the PTO system on board the prototype MWP device, the model will enable future design improvements on the current system. For example, questions such as the effect of different sized accumulators, or even just the effect of a different precharge pressure in the accumulator, can be answered. However, the motivation behind producing the PTO model was to assist in future control design. The current model will allow this to be done, facilitating all possible PTO control inputs. The model also enables calculation of the damping force supplied by the PTO on the wave barge motion. Further discussion on this is in section 4.1.

3.7 PTO System Notation

c	: Rotational damping coefficient
C	: Translational damping coefficient
C_{acc}	: Accumulator capacitance
v_0	: nominal volume of accumulator
p_0	: nominal pressure of accumulator
Q_{tv}	: flow from control valve
γ	: ratio of specific heats
f	: friction factor
V	: velocity of fluid in pipe
g	: acceleration due to gravity
L	: length of pipe
D	: diameter of pipe
K	: resistance coefficient
Q_w	: rate of water flow through membrane
$\triangle P$	: pressure across membrane
$\triangle P_{osm}$	: osmotic pressure across membrane
K_w	: membrane permeability coefficient
S	: membrane area
d_m	: membrane thickness
V_j	: fluid jet velocity
ρ	: fluid density
p_1	: pressure across control valve
P_h	: hydraulic power
Q_{tv}	: flow through control valve

4 Coupling of the PTO and MWP/Wave Systems

In this section, we consider the interconnection of the wave/barge model reported on in Section 2 and the power take-off model developed in Section 3. This becomes an issue, since the PTO system effectively 'loads' the MWP, with an exchange of damping and driving forces, as illustrated in Figure 7.

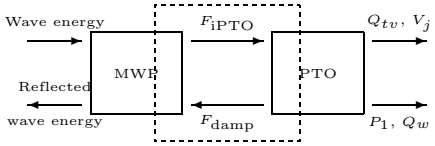

Figure 7: Coupling between MWP and PTO

4.1 Damping effect of PTO on MWP

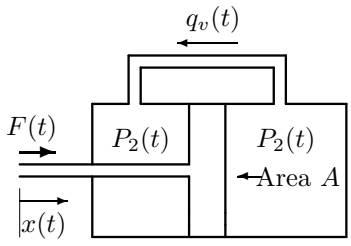

Figure 8: Damping coefficient calculation

Considering a single pump (non-restrictive) as shown in figure 8, we can write the effective damping force as:

$$F(t) = C\frac{dx(t)}{dt} \tag{11}$$

where C is the effective translational damping coefficient. However,

$$q_v(t) = A\frac{dx(t)}{dt} \quad or \quad \frac{dx(t)}{dt} = \frac{q_v(t)}{A} \tag{12}$$

and

$$[P_1(t) - P_2(t)] = \Delta p = \frac{F(t)}{A} \tag{13}$$

giving:

$$C(t) = \frac{A^2\Delta p(t)}{q_v(t)} \tag{14}$$

allowing $C(t)$ to be dynamically calculated from the PTO variables ($\Delta p(t)$ and $q_v(t)$) at each point in time.

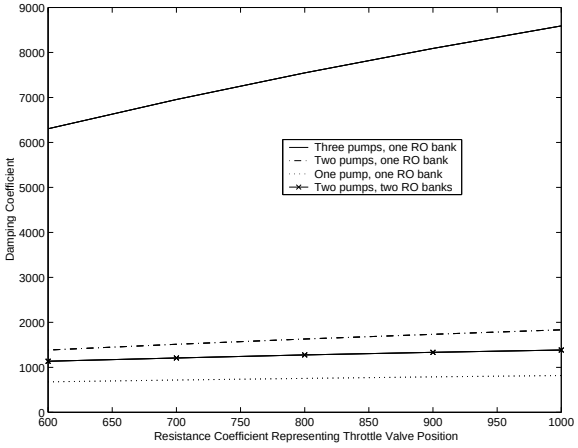

Figure 9: Damping Coefficient

Note that $C(t)$ is a constant for a given throttle valve position if the accumulator is removed (see, for example, Fig.9).

4.2 Driving force from MWP

This is calculated by solving the dynamical equations for the MWP, which returns values for θ_i and $\dot{\theta}_i$. The rotational and, finally, translational forces are then calculated via equations (2) and (3) respectively.

4.3 Coupling of MWP and PTO

Clearly, the driving force from the MWP must be equal and opposite to the damping force supplied by the PTO. This leads to a sense that both systems must be modelled using an integrated approach and the bond graph method provides an

ideal framework for this through its use of energy links, which easily encompasses the concept of 'loading'. However, the hinge-barge model developed in [1] was not developed within such a framework and, while recasting of the model in a bond graph form may theoretically be feasible, the high dimensionality of the hinge-barge model coupled with the further increase in the dimension of the equation set typical of the bond-graph approach precludes such an approach. A reasonable approximation is provided by the following:

1. The damping factor for the PTO is initialised using the static TV_p/C characteristic as shown in Fig. 9

2. The hinge-barge equations are solved for this value of C

3. The driving force on the pumps from the hinge-barge is now calculated ($F_{i_{PTO}}$) and the PTO equations solved

4. A new 'effective' PTO C is now calculated. Goto Step 2.

5 Control System Formulation

In order to set the context of the control problem, the system inputs and outputs are documented in Tables 1 and 2.

Input	Notation
Pos. of throttle valve	p_{tv}
Ballast quantity and position	(M_{bal},P_{bal})
Number of pumps employed	N_{pumps}
Number of RO sections employed	N_{RO}

Table 1: System inputs

Output	Notation
Flow of potable water	Q_w
Throttle valve flow	Q_{tv}
Throttle valve jet velocity	V_j
Angles and velocities of MWP	θ_i, $\dot{\theta}_i$

Table 2: System outputs

The MWP, and associated PTO system, represents a nonlinear, multivariable control problem. Nonlinearity appears in the wave/body interactions (see Section 2.3), but most prominently in the damping term, via the PTO system. In particular, the throttle valve position, TV_p, representing the primary control input, ultimately appears as a *parameter* in the MWP dynamical equations, rather then a variable. In addition to this significant nonlinearity, the ability to switch between different numbers of pumps and RO sections puts the problem within the realms of switching systems [16], where care must be taken to ensure that stability and nominal performance is maintained across switching boundaries. The control problem may be formulated as a constrained optimisation problem:

Maximise:

$$J(u) = \int_{t=0}^{\infty} (Q_w(t) + \beta P_h(t))dt \tag{15}$$

subject to:

$$|\theta_1| < \theta_1(max), |\theta_2| < \theta_2(max), |\theta_3| < \theta_3(max) \tag{16}$$

where the control input vector is formed as:

$$u = [p_{tv}, N_{pumps}, N_{RO}, M_{bal}, P_{bal}]^T \tag{17}$$

There may also be constraints on $\dot{\theta}_i$ and also possibly on accelerations. The equation set above can be solved using numerical optimisation. However, this is not very elegant in exploiting the particular structure of the MWP/PTO model and some difficulty is likely to be experienced with local minima. Nevertheless, considerable research is currently going into improving optimisation methods for control design [17, 18] and the relatively slow dynamics (with consequent length sampling period) of the MWP permits significant computation, including numerical optimisation, in the computation of the control law.

6 Conclusions

This paper has addressed the development of an integrated mathematical model of the MWP/PTO system, with a view to providing a basis for model-based control design. Clearly, there are some significant challenges in the resulting control problem, due mainly to the dependence of system parameters on operating variables and other nonlinearity. Future efforts will focus on the validation of the model structure and parameter values for the prototype MWP rig in tandem with progressing the control design itself.

Acknowledgement

The authors are grateful for the contribution of Prof. Peter Wellstead of the Hamilton Institute at NUI Maynooth, who gave unselfishly of his time and cleared up many points relating to the use of bond graphs.

References

[1] Kraemer, D.R.B. The motions of hinged-barge systems in regular seas. PhD. Thesis, Johns Hopkins University, 2001.

[2] Kraemer, D.R.B, Ohl, C.O.G, & McCormick, M.E. Comparison of experimental and theoretical results of the motions of a McCabe Wave Pump, Proc. 4th European Wave Energy Conference, Aalborg University, Denmark, 2000.

[3] McCormick, M.E. A normal-mode analysis of the critically damped motions of hinged barges in regular long-crested waves. Journal of Ship Research, Vol.31(2), pp91-100, 1987.

[4] McCormick, M.E. & Ohl, C.O.G. An experimental study of the motions of the McCabe Wave Pump, Technical Report EW-27-96, US Naval Academy, Annapolis, MD,USA, December 1996.

[5] McCormick, M.E., Murtagh, J. & McCabe, P. Large-scale experimental study of a hinged-barge wave energy conversion system, Proc. 3rd European Wave Energy Conference, Patras, Greece, 1998.

[6] Murtagh, J. Private Correspondence, 2002

[7] Newman, J.N. Marine Hydrodynamics, MIT Press, 1977.

[8] Jefferys, E.R. Simulation of wave power devices, Applied Ocean Research, Vol.6, pp 31-39, 1984.

[9] Yu, Z. & Falnes, J. State-space modelling of a vertical cylinder in heave, Applied Ocean Research, Vol.17, pp 265-275, 1995.

[10] Murtagh, J. Private Correspondence. 2003.

[11] Samantaray, A.K., About bond graphs and application notes [online]. Available from: http://www.bondgraphs.com [Accessed Febuary 2003].

[12] Istif, L., Sagirli, A. & Kutlu, K. Bond graph modelling and position control of an electrohydraulic elevator, Proc. 6th Biennel Conference on Engineering Systems Design and Analysis, Istanbul, Turkey, 2002.

[13] College of Engineering and Technology, Brigham Young University. Dynamic system modelling lecture notes [online]. Available from: http://class.et.byu.edu/me435-3/ [Accessed March 2003].

[14] Hydraunautics. Terms and equations of reverse osmosis [online]. Available from: http://www.itpapers.com [Accessed March 2003].

[15] Darcy, H. Recherches Experimentales Relatives au Mouvement de L'Eau dans les Tuyaux ("Experimental Research Relating to the Movement of Water in Pipes"), Mallet-Bachelier, Paris, 1857.

[16] Liberzon, D. and Morse, A.S. Basic problems in stability and design of switched systems, IEEE Control Systems Magazine, Vol.19, No.5, pp 59-70, Oct. 1999.

[17] Balakrishnan, V., Wang, F. and Vandenberghe, L. Applications of semidefinite programming in process control Proc. American Control Conference, Vol.5, June 2000, pp 3219-3223.

[18] Rao C.V. and Rawlings J.B. Linear programming and model predictive control, J. Process Control, Vol.10 No.2-3, 2000, pp 283-289.